THE AMERICAN SOCIETY OF MECHANICAL ENGINEERS
345 E. 47th St., New York, N.Y. 10017

94-GT-312

FILM COOLING WITH COMPOUND ANGLE HOLES: ADIABATIC EFFECTIVENESS

Donald L. Schmidt, Basav Sen, and David G. Bogard
Mechanical Engineering Department
University of Texas at Austin
Austin, Texas

ABSTRACT

Film cooling effectiveness was studied experimentally in a flat plate test facility with zero pressure gradient using a single row of inclined holes which injected high density, cryogenically cooled air. Round holes and holes with a diffusing expanded exit were directed laterally away from the freestream direction with a compound angle of 60°. Comparisons were made with a baseline case of round holes aligned with the freestream. The effects of doubling the hole spacing to six hole diameters for each geometry were also examined. Experiments were performed at a density ratio of 1.6 with a range of blowing ratios from 0.5 to 2.5 and momentum flux ratios from 0.16 to 3.9. Lateral distributions of adiabatic effectiveness results were determined at streamwise distances from 3 D to 15 D downstream of the injection holes. All hole geometries had similar maximum spatially averaged effectiveness at a low momentum flux ratio of I = 0.25, but the round and expanded exit holes with compound angle had significantly greater effectiveness at larger momentum flux ratios. The compound angle holes with expanded exits had a much improved lateral distribution of coolant near the hole for all momentum flux ratios.

NOMENCLATURE

CA = compound angle
D = film cooling hole diameter
DR = density ratio of coolant to mainstream = ρ_c/ρ_∞
H = shape factor = δ_1/δ_2
I = momentum flux ratio of coolant to mainstream = $\rho_c U_c^2/\rho_\infty U_\infty^2$
L = hole length
M = mass flux ratio of coolant to mainstream = $\rho_c U_c/\rho_\infty U_\infty$
P = hole spacing
Re = Reynolds number
T = temperature
U = streamwise velocity
x = streamwise coordinate originating at downstream edge of cooling holes
z = spanwise coordinate originating at centerline of central hole
β = angle of injection with respect to the surface
δ_1 = displacement thickness
δ_2 = momentum thickness
η = adiabatic effectiveness = $(T_{aw} - T_\infty)/(T_c - T_\infty)$
ρ = density

Subscripts

aw = adiabatic wall
c = coolant
∞ = freestream

Superscripts

$\bar{}$ = lateral average
$=$ = spatial average

INTRODUCTION

Discrete hole film cooling is an important technique for cooling turbine blades in gas turbine engines. Much of the published research on the effectiveness of film cooling has concentrated on round holes, inclined at approximately 35° with respect to the surface, and aligned with the mainstream flow. In this work we used a flat plate test facility with zero pressure gradient to study the effectiveness of a single row of holes directed laterally away from the mainstream direction (i.e. with a non-zero compound angle). Two sets of laterally

Presented at the International Gas Turbine and Aeroengine Congress and Exposition
The Hague, Netherlands — June 13–16, 1994

directed holes were studied, the first had round holes and the second had holes with a circular metering section and a diffusing forward expansion at the exit of the holes (forward expanded holes).

Compound angle injection has received renewed attention because this orientation is "believed to produce injectant distributions over surfaces giving better protection and higher film effectivenesses than injectant from holes with simple angle orientations" (Ligrani, Ciriello, and Bishop, 1992). However, there are few experimental or computational studies reported in the open literature. Experimental adiabatic effectiveness studies of laterally directed injection from a single row of holes into a zero pressure gradient flow over a flat plate are limited to those by Goldstein, Eckert, Eriksen, and Ramsey (1970) for a single round hole with $\beta = 15°$ and 35°, CA = 90°; Ligrani et al. (1992) for a single row of round holes with $\beta = 24°$, CA = 50.5°; and Honami, Shizawa, and Uchiyama (1992) for a single row of round holes with $\beta = 30°$, CA = 90°. Honami et al. did not include streamwise directed holes as a basis for comparison, but their near-hole compound angle effectiveness behavior was comparable to the other two studies. Compared to streamwise directed jets, the lateral spread of a compound angle film cooling jet increased, thus improving the laterally averaged effectiveness near the injection location. A significant improvement over streamwise directed jets was found at higher blowing ratio, $M \geq 1$ (all these studies were done at density ratio of $DR \approx 1$, so this corresponds to $I \geq 1$), which indicated that the jets stayed closer to the wall when a compound angle was used. However, far downstream the effectiveness results were different at higher M. Goldstein et al. (1970), who determined effectiveness from adiabatic wall temperature measurements, found that the improvement was sustained far downstream. Ligrani et al. (1992), who deduced adiabatic results from Stanton number extrapolations using superposition, found that the compound angle effectiveness decreased to the values for CA = 0° holes over a similar streamwise distance.

A computational study of a single row of laterally directed holes was conducted by Sathyamurthy and Patankar (1990), for a streamwise distance to x/D = 10 downstream of the holes. Rows of holes with $\beta = 30°$, CA = 45° and 90°, and with spacing between holes from P/D = 3 to 5 were investigated with unit density ratio injection. They stated that their analysis should be interpreted as qualitative since there is very limited experimental data with which to validate the computations. For P/D = 3 and M = 1.0 (I = 1.0), the laterally averaged effectiveness was found to improve with increase in compound angle, but at P/D = 5 there was very little difference for CA = 0°, 45°, or 90°. They also found that for laterally directed holes the average effectiveness continued to increase with increase in blowing ratio up to M = 3.0 (I = 9.0), the maximum blowing ratio computed.

The shape of the film cooling hole is also an important geometric variable, but it has received limited attention in the literature. Goldstein, Eckert, and Burggraf (1974) examined holes which had circular metering sections and were widened

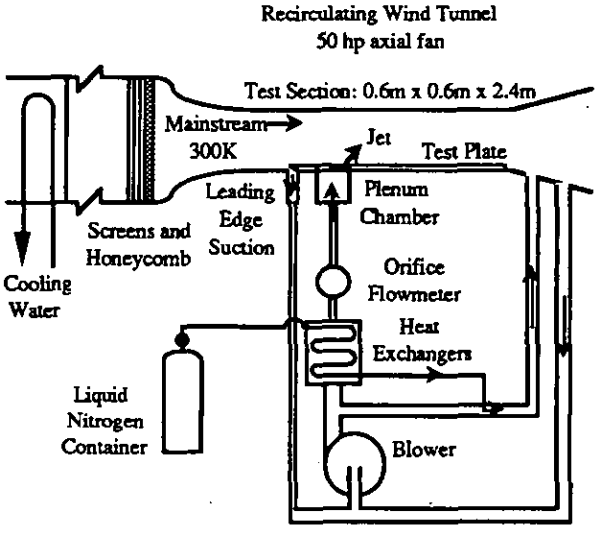

FIGURE 1. Film cooling test facility.

out at 10° near the exits. Makki and Jakubowski (1986) examined holes which had trapezoidal cross sections and were diffused in the direction of the mainstream flow. They used a transient facility, for which film cooling performance was indicated by the ratio of heat transfer coefficients with cooling to without cooling. Both studies showed that expanding the hole exit improved film cooling performance compared to the round hole base case. However, there are no studies of the effects of compound angle with shaped or expanded holes in the open literature.

The effects of increasing hole spacings were discussed by Brown and Saluja (1979) and Foster and Lampard (1980) for streamwise directed holes. Spacing of injection holes affects film cooling performance in two ways: the spacing determines the coolant mass per unit span at a given blowing condition, and closer spacing promotes jet merging, thus improving lateral coverage. There have been no studies reported for compound angle holes.

The customary way to describe film cooling performance defines the heat transfer coefficient in terms of adiabatic wall temperature, T_{aw}. In non-dimensional form, T_{aw} is expressed as the adiabatic effectiveness. In the present experimental program, adiabatic effectiveness and heat transfer coefficients were determined for laterally directed film cooling holes, round and expanded, and for round streamwise directed holes (as a basis for comparison). This paper presents the adiabatic effectiveness results. The associated heat transfer coefficients for the different hole configurations are presented in Sen, Schmidt, and Bogard (1994).

EXPERIMENTAL FACILITIES AND TECHNIQUES

Experiments were conducted in a closed loop, subsonic wind tunnel facility, illustrated in Figure 1. A secondary flow loop provided cryogenically cooled injection air to obtain the desired density ratio. Further details of the facility can be

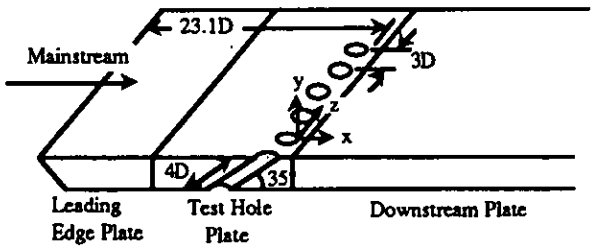

FIGURE 2. Test section geometry and coordinate system.

found in Pietrzyk, Bogard, and Crawford (1990). The flat test plate was a modular design composed of three sections: a 12.7 cm long, sharp leading edge plate; a 14 cm long injection plate; and an instrumented downstream plate. The injection plate had a single row of holes with specified geometric parameters. The geometry and coordinate system of the film cooled test plate is shown in Figure 2.

This study considered three hole geometries, illustrated in Figure 3, all with injection angle $\beta = 35°$, metering diameter D = 11.1 mm, and a hole length of L = 4 D. The test plates were constructed from extruded polystyrene foam (STYROFOAM) with 9 holes at a hole spacing of 3 D; hole spacing was doubled by taping alternate holes closed. Two compound angles were used: a CA = 0°, with the hole axes aligned with the freestream direction; and a CA = 60°, with the hole axes at a 60° angle to the freestream. The CA = 0° holes were round holes and were tested as a basis of comparison. Two geometries were constructed with CA = 60°: a round hole case and a forward expanded exit case. The metering length, measured along the hole axis, was 2.1 D for the expanded exit holes, and the exit was expanded at a 15° angle along the line of the laterally directed hole as indicated in Figure 3. Note that the projected cross-stream exit width of the expanded hole with CA = 60° was 3.3 D, which resulted in an overlapping of the projected widths, although the holes did not physically overlap. The hole inlets and exits were sharp edged, and the interiors were aerodynamically smooth.

The downstream plate was constructed from STYROFOAM to provide an adiabatic boundary condition. A three dimensional conduction heat transfer code indicated negligible conduction errors for this plate material (Sinha, Bogard, and Crawford, 1991). The foam was bonded to a fiberglass composite (EXTREN) for structural rigidity. Below the EXTREN were 15.2 cm of Corning fiberglass insulation and 2.54 cm of STYROFOAM. The downstream plate had an array of thin ribbon thermocouples epoxied to the surface for surface temperature measurements. The thickness of a thermocouple junction was measured and found to be less than 0.09 mm, which corresponded to a turbulent boundary layer measurement for the near wall region of $y^+ < 5$. This was more than an order of magnitude greater than the surface roughness of the STYROFOAM, which was measured to be less than 0.005 mm. Consequently the surface was aerodynamically smooth.

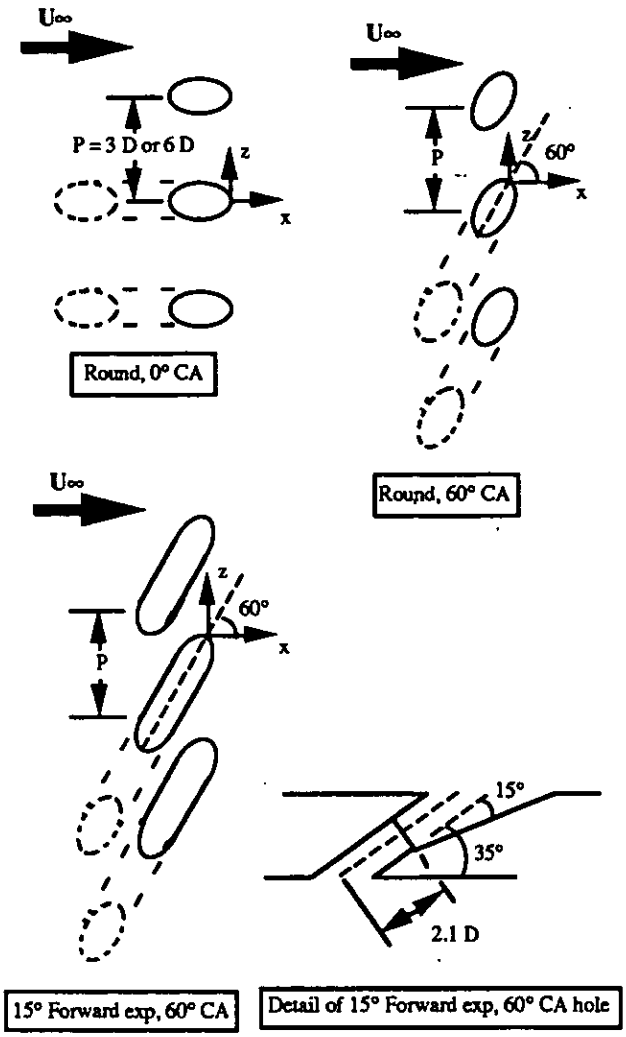

FIGURE 3. Injection hole geometry showing the top view of the central three holes for all three geometries, and details of the geometry for the 15° forward expansion, 60° CA holes.

The thermocouple ribbons were connected to thermocouple extension wires below the plate surface, and the wires were routed through the EXTREN base plate. Further details on the thin ribbon thermocouple design are provided in Sinha et al. (1991). Nine thermocouple junctions were located on the central hole centerline from 2 D to 30 D downstream of the trailing edge of the hole. Seven thermocouple junctions spanned the lateral distance from -1.5 D to +1.5 D at streamwise locations of 3 D, 6 D, 10 D, and 15 D. These lateral locations were for P/D = 3 hole spacing. For P/D = 6 spacing two runs were necessary to form a composite picture of the cooling jet performance. In these cases, with the central hole open and adjacent holes taped data was obtained for $-1.5\ D \le z \le 1.5\ D$, and with the central hole taped and adjacent holes open data was obtained for $1.5\ D \le z \le 4.5\ D$. Thermocouples were used to monitor freestream and secondary loop

temperatures. Acquisition of temperature data and data processing was automated to allow on-line analysis of film cooling effectiveness. Pressure differentials across the wind tunnel contraction and across a sharp-edged orifice plate in the secondary flow loop were used to set freestream velocity and injection flow rate, respectively.

The operating technique utilized for this study was to set the mass flow rate of the cryogenically cooled injectant, then vary the freestream velocity to obtain the desired blowing conditions. The freestream velocity ranged from $U_\infty = 30$ m/s to 7.5 m/s, providing momentum flux ratios from I = 0.16 to 3.9 (M = 0.5 to 2.5), with DR = 1.6. A comprehensive description of freestream and boundary layer development and uniformity was given in Pietrzyk et al. (1990) for a 20 m/s freestream velocity. The boundary layer was measured to be a fully developed turbulent boundary layer at $U_\infty = 20$ m/s and $U_\infty = 10$ m/s. For $U_\infty = 20$ m/s, the boundary layer parameters were, $Re_{\delta 2} = 1100$, $\delta_1/D = 0.120$, and H = 1.48, respectively. At $U_\infty = 10$ m/s, the boundary layer parameters were $Re_{\delta 2} = 700$, $\delta_1/D = 0.151$, and H = 1.46. The precision uncertainty on freestream velocity was $\delta U_\infty = \pm 1\%$, and the freestream turbulence level was about Tu = 0.2%. The Reynolds number based on the freestream velocity and the hole diameter ranged from $Re_D = 5000$ to 21000. The technique of varying freestream conditions to obtain the various I and M ratios raised concerns about Reynolds number effects. Tests were conducted maintaining a constant I using several injectant mass fluxes and freestream velocities for one geometry at one low I near the optimum performance condition, and one high I. The variation in the laterally averaged effectiveness was within the uncertainty of $\bar{\eta}$ for injection conditions spanning the experimental range.

Pietrzyk et al. (1990) also documented the film cooling loop. The cooling jets were supplied by a common plenum. Pietrzyk et al. performed laser Doppler anemometry measurements of individual jets and found a mean velocity variation between jets of $\delta U_c = \pm 2.6\%$. For the data described below, the mass flux ratio was held constant within $\delta M = \pm 4\%$ during experiments. The injectant-to-freestream density ratio was DR = 1.6. Maximum variation of density ratio during the experiments was $\delta DR = \pm 4\%$. The variation in density ratio was primarily due to variation in fluid temperatures during the runs.

The low temperature of the dense jets meant a potential for H_2O and CO_2 to solidify and accumulate in the secondary flow loop and on the test plate. Wind tunnel air drying techniques and operating procedures developed by Pietrzyk et al. (1990) to reduce the frosting potential were employed. A new heat exchanger for cooling the jets was installed and the tunnel was sealed to minimize air infiltration to the wind tunnel, although a fully effective seal could not be obtained. This meant that frost could accumulate during an experiment, and it would have to be removed from the test plate between adiabatic effectiveness measurements. Repeated tests showed consistent performance was obtained after frost removal, with the variation in local effectiveness, laterally averaged effectiveness, and spatially averaged effectiveness being $\delta\eta = \pm 0.01$, $\delta\bar{\eta} = \pm 0.01$, and $\delta\bar{\bar{\eta}} = \pm 0.01$, respectively.

The overall uncertainty in effectiveness measurements was dominated by run-to-run variations. Although the total injectant mass flow was the same, the run-to-run mean velocity variation for an individual jet was the same as the mean velocity variation between jets. The variation was believed to be due to variations in frost accumulation around the film cooling hole entrances, which would have altered the flow dynamics from one experiment to the next, resulting in slight differences in momentum flux ratio, I, from run-to-run. The variation was not a big factor at low I, where the jets were attached to the surface anyway. However, the variation in flow rate was a big factor at high I, where the condition of jet attachment was sensitive to I. At blowing conditions $I \leq 0.9$, the uncertainties in effectiveness measurements were $\delta\eta = \pm 0.03$, $\delta\bar{\eta} = \pm 0.03$, and $\delta\bar{\bar{\eta}} = \pm 0.02$. At higher blowing conditions, the uncertainties were $\delta\eta = \pm 0.08$, $\delta\bar{\eta} = \pm 0.06$, and $\delta\bar{\bar{\eta}} = \pm 0.05$. In terms of percentages, these uncertainties represent 7% of the peak values of η, $\bar{\eta}$, and $\bar{\bar{\eta}}$ at lower I, and approximately 20% of the peak values at higher I.

The evaluation of film cooling performance discussed below refers to blowing ratio and momentum flux ratio. These ratios are defined using the injectant velocity, U_c, based on the flow rate and the cross section area of the metering length of the hole. Studies reported in the literature commonly use the jet velocity in the definitions of M and I. However, expanding the hole exit increases the cross section area after the metering length, hence the jet velocity decreases. In this situation, U_c is used in the description of flow conditions since the correct representative jet velocity is not known.

RESULTS AND DISCUSSION

Results for the three hole geometries tested are presented in terms of lateral variations of local effectiveness η, streamwise variation of laterally averaged effectiveness $\bar{\eta}$, and finally the variation of spatially averaged effectiveness $\bar{\bar{\eta}}$ as a function of momentum flux ratio. The results of the 3 D and 6 D hole spacings are presented together to aid in the description of the effects of compound angle injection. For the coordinate system we placed the streamwise coordinate origin, x = 0, at the trailing edge of the film cooling hole. The lateral coordinate origin, z = 0, was at the centerline of the trailing edge of the central hole. The coordinate system origins are shown in Figure 3 for each geometry.

The validity of the round hole CA = 0° results was established by comparing the effectiveness with results from Pedersen, Eckert, and Goldstein (1977) and results from Sinha et al. (1991). Both studies had injection geometries similar to the present study and measured effectiveness at high density ratio. For low I, there was good agreement between the present results and the data of Pedersen et al. and Sinha et al., as illustrated by the centerline data in Figure 4(a). At high I (Figure 4(b)), for which jet lift-off occurs in the near-hole region, the present results showed some deviation from the

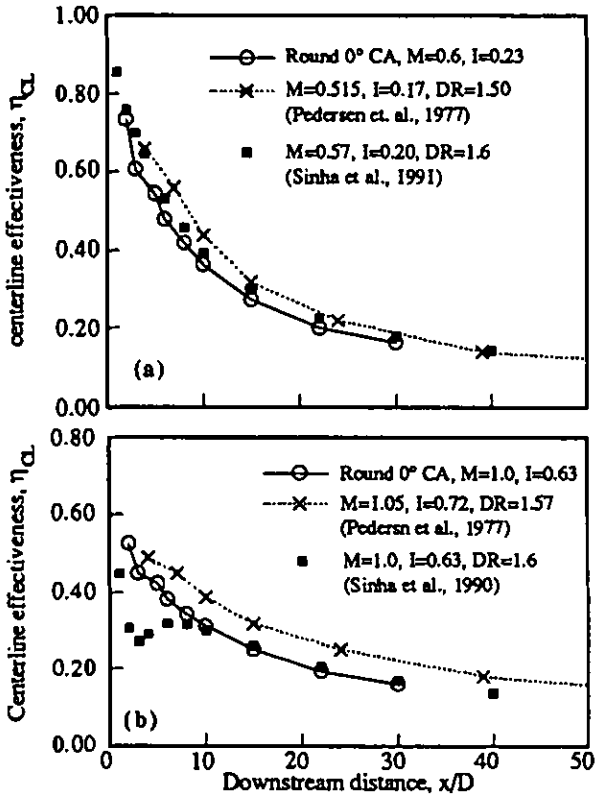

FIGURE 4. Comparison of round hole centerline effectiveness to published data (a) I = 0.23, M = 0.6, (b) I = 0.63, M = 1.0.

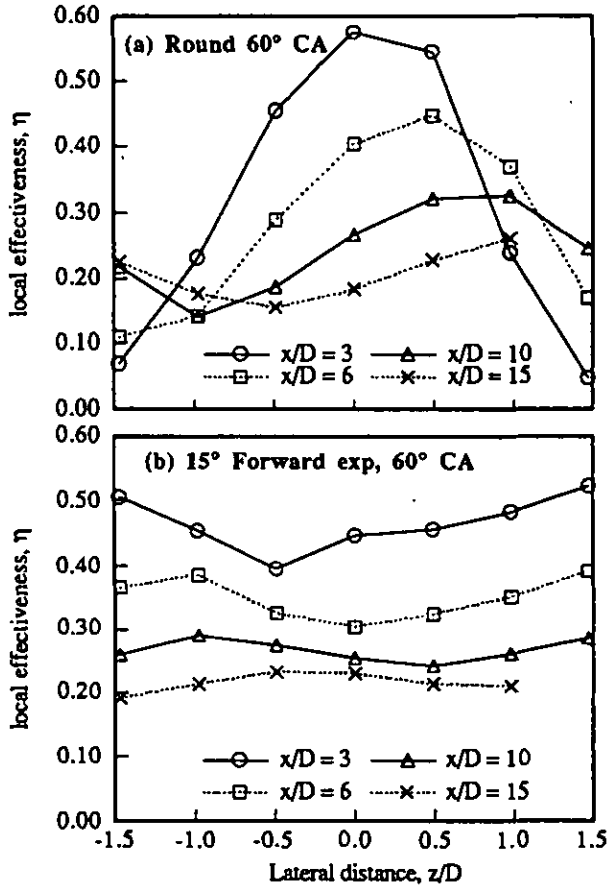

FIGURE 5. Local lateral effectiveness for the holes with CA = 60°, I = 0.25, M = 0.63 (a) round holes with CA = 60°, (b) expanded holes with CA = 60°.

data of Pedersen et al. and Sinha et al. The difference was primarily attributed to differences in the film cooling hole length-to-diameter ratio for the different studies.

The lateral movement of the cooling jet expected for compound angle injection is clearly illustrated in Figure 5 (a), which shows lateral η distributions at the four streamwise stations for the round hole with CA = 60°. A distinct difference in the initial lateral distribution of coolant for the round holes and expanded exit holes with compound angle is evident when comparing Figures 5 (a) and (b). The expanded exit holes have an almost uniform lateral distribution of coolant at the first measurement position of x/D = 3, while the round holes show show a large lateral variation. However, by x/D = 15 both round and expanded exit holes with compound angle show similar uniform lateral distributions.

We selected x/D = 10 as a representative position for the following comparisons of of the lateral distribution of η for the different hole geometries. Results presented in Figure 6 are representative of low momentum flux ratio (I < 0.5), and results presented in Figure 7 are representative of high momentum flux ratio (I > 1.0). Figure 6 (a) shows that η > 0.1 across the span between holes for low I and for P/D = 3. This result suggests that there is some merging of the coolant jets for all hole geometries for this hole spacing. For P/D = 6, Figure 6 (b) shows distinct region of zero effectiveness indicating the coolant jets no longer merged (note data was not taken for z/D > 1.5 for round CA = 0° and the round CA = 60° holes because it was evident that η would be essentially zero over this range). Also evident from Figure 6 (b) is that the forward expanded CA = 60° holes deliver a much greater lateral distribution of the coolant. At high I, Figure 7 (a) shows that the round and the forward expanded CA = 60° holes have similar good lateral distribution of coolant for P/D = 3, and both are clearly superior to the round CA = 0° holes. However, for P/D = 6, Figure 7 (b) shows regions of zero effectiveness indicating that the coolant jets have not merged, but there is a greater lateral distribution of coolant for both the round and forward expanded compound angle holes. Note that in Figure 7 (b) both compound angle cases also exhibited steep η gradients on the side toward which the jets were directed. We attribute this to the impact of the mainstream on this side of the jet causing a sharp shear layer.

Laterally averaged effectivenesses were determined by integrating the measured lateral distribution of η and dividing by the span between hole centerlines. A simple trapezoidal

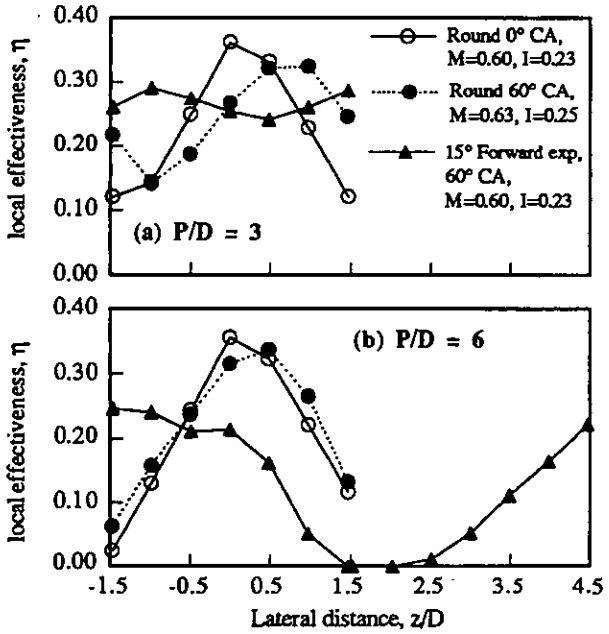

FIGURE 6. Local lateral effectiveness at x/D = 10 for the test holes, I ≈ 0.25, M ≈ 0.6 (a) P/D = 3, (b) P/D = 6.

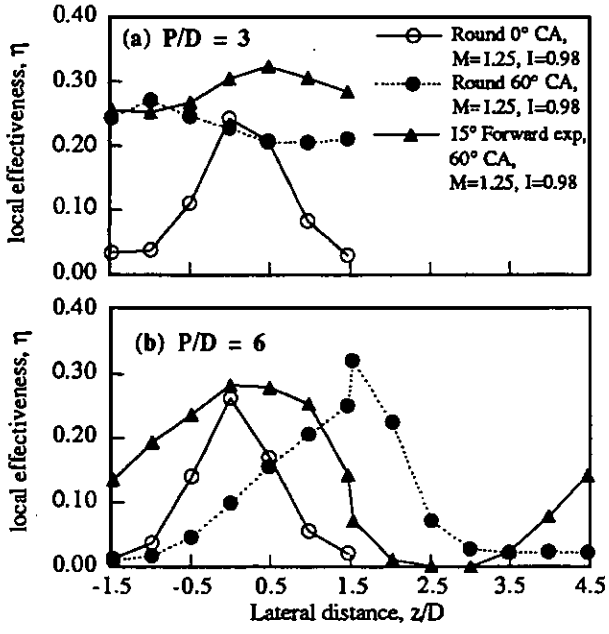

FIGURE 7. Local lateral effectiveness at x/D = 10 for the test holes, I = 0.98, M = 1.25 (a) P/D = 3, (b) P/D = 6.

integration was used since it was found to give the same result as higher order polynomial fits. Results are shown as a function of downstream distance for I = 0.25 and I ≈ 1.0 in Figures 8 and 9, respectively. At the lower I, adding a

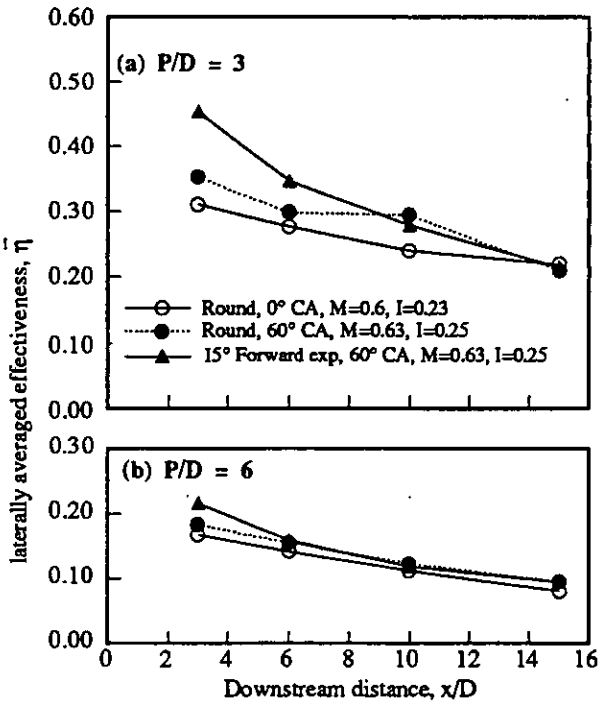

FIGURE 8. Laterally averaged effectiveness for the test holes, I ≈ 0.25, M ≈ 0.6 (a) P/D = 3, (b) P/D = 6.

compound angle to the round hole did not significantly change $\bar{\eta}$ compared to the base case round hole. In contrast, the combination of compound angle with the forward expanded exit caused a significant increase immediately downstream of the hole, but fell to a level equivalent to the round holes by x/D = 10. The initial improved $\bar{\eta}$ value for the forward expanded CA = 60° may be attributed to the improved lateral distribution of the coolant discussed previously. Increasing the spacing between holes from P/D = 3 to P/D = 6 caused approximately a factor of two decrease in $\bar{\eta}$, and $\bar{\eta}$ values for each of the holes were very similar.

Figure 9 shows that at relatively high I, there were distinct differences in the effectiveness for the different hole geometries. Both compound angle holes had significantly greater effectiveness than the baseline case round hole with CA = 0°. This is mainly because of a large decrease in $\bar{\eta}$ for the CA = 0° round hole, which may be attributed to detachment of the cooling jet from the surface. Detachment of the cooling jet for CA = 0° round holes at I = 1.0 is consistent with results of Thole, Sinha, Bogard, and Crawford (1992) who showed that the coolant jet would be fully detached for I > 0.8. Again the forward expanded exit with CA = 60° significantly increased $\bar{\eta}$ immediately downstream of the holes, but fell to a level comparable to the round CA = 60° holes by x/D = 15. When the hole spacing was doubled, $\bar{\eta}$ was reduced by a factor of two, but the CA = 60° geometries retained significantly increased effectiveness relative to the CA = 0° holes.

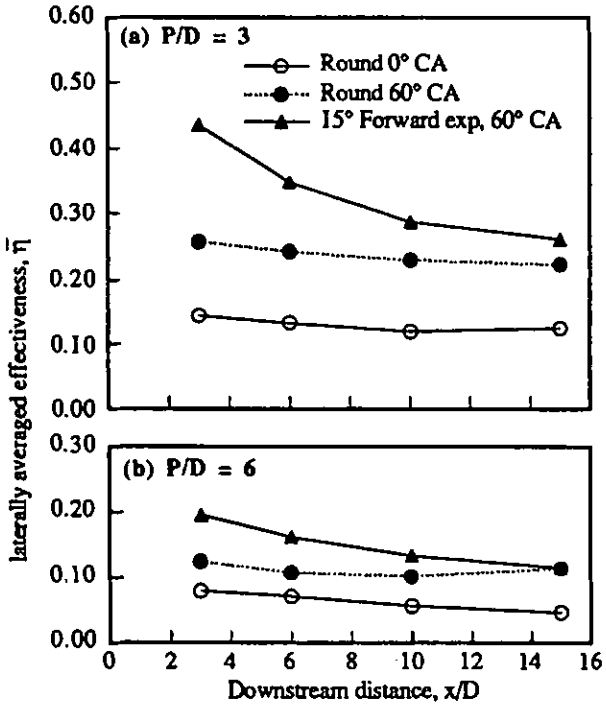

FIGURE 9. Laterally averaged effectiveness for the test holes, I = 0.98, M = 1.25, (a) P/D = 3, (b) P/D = 6.

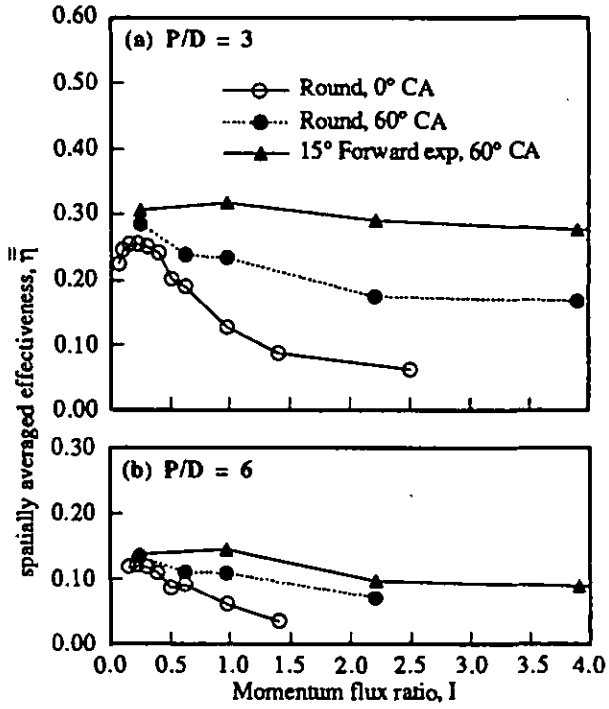

FIGURE 10. Spatially averaged effectiveness for the test holes (a) P/D = 3, (b) P/D = 6.

To compare the effectiveness of the different geometries over a full range of momentum flux ratios a spatially averaged adiabatic effectiveness, $\bar{\bar{\eta}}$, was used. This quantity was defined as the integral average of the laterally averaged effectiveness from x/D = 3 to 15. Results for $\bar{\bar{\eta}}$ for all three geometries as a function of momentum flux ratio are shown in Figure 10. Immediately obvious from Figure 10 (a) for P/D = 3 is that the effectiveness at low I is very similar for the different geometries, but adding a 60° compound angle significantly increased the range over which high effectiveness levels were maintained. The forward expanded exit holes with CA = 60° maintained essentially the same level of $\bar{\bar{\eta}}$ over the full range tested, 0.25 < I < 3.9, and were significantly better than the round CA = 60° holes at the larger I. For the round CA = 60° holes, $\bar{\bar{\eta}}$ decreased slightly with increasing I, but still had reasonably good effectiveness at I = 3.9. This decreasing trend for the CA = 60° round holes is somewhat different than the computational predictions of Sathyamurthy and Patankar (1990) which indicated a constant level of effectiveness for CA = 45° round holes, and increasing effectiveness with increasing I for CA = 90° round holes.

The effect of increasing hole spacing to P/D = 6 is shown in Figure 10 (b). The results are somewhat similar to the P/D = 3 results with the $\bar{\bar{\eta}}$ levels generally decreased by a factor of two. Results for the round holes with CA = 0° and CA = 60° can be compared with the results of Ligrani et al. (1992), who used round holes with CA = 0° and CA = 50.5°, but with an injection angle of β = 24°. The magnitudes of the effectiveness deduced from Ligrani et al.'s data over the range x/D = 5 to 15 were very similar to the present results for the range that Ligrani et al. tested, 0.25 < I < 2.2. Similarly they found that that the effectiveness of the compound angle round holes decreased with increasing I, but improved relative to the CA = 0° holes.

CONCLUSIONS

All three geometries had very similar spatially averaged adiabatic effectiveness at low momentum flux ratio, although the forward expansion with CA = 60° holes had an improved lateral spread of the film cooling jets immediately behind the holes. Adding a compound angle to the baseline round hole geometry significantly improved effectiveness at high momentum flux ratios, and the combination of compound angle and forward expansion provided further improvement. With a hole spacing of P/D = 3, the forward expanded CA = 60° holes maintained essentially the same level of spatially averaged effectiveness for the range of I studied, while the round CA = 60° holes effectiveness level decreased slightly with increasing I. The higher spatially averaged effectiveness obtained for the forward expanded holes was due to significantly higher effectiveness very near the hole, but by x/D = 15 the forward expanded and round CA = 60° holes had essentially the same effectiveness. With P/D = 6, both compound angle geometries retained significantly improved effectiveness compared to the streamwise directed round holes.

These results indicate that film cooling with compound

angle injection does not provide higher adiabatic effectiveness, but does provide high effectiveness over a considerably larger range of momentum flux ratios. However, these adiabatic effectiveness results must be coupled with the heat transfer coefficients to determine overall performance as discussed in Sen et al. (1994).

ACKNOWLEDGMENT

The authors gratefully acknowledge Garrett Engine Division of the Allied-Signal Aerospace Company and the Air Force Wright-Patterson Research and Development Center for support of this research. We would also like to thank Mr. Noor Sait, Mr. David Dotson, and Dr. Karen Thole for their assistance in conducting experiments.

REFERENCES

Brown, A., and Saluja, C. L., 1979, "Film Cooling From a Single Hole and a Row of Holes of Variable Pitch to Diameter Ratio," *International Journal of Heat and Mass Transfer*, Vol. 22, pp. 525-533.

Goldstein, R. J., Eckert, E. R. G., and Burggraf, F., 1974, "Effects of Hole Geometry and Density on Three-Dimensional Film Cooling," *International Journal of Heat and Mass Transfer*, Vol. 17, pp. 595-607.

Goldstein, R. J., Eckert, E. R. G., Eriksen, V.L., and Ramsey, J.W., 1970, "Film Cooling Following Injection Through Inclined Circular Tubes," *Israel Journal of Technology*, Vol. 8, pp. 145-154.

Honami, S., Shizawa, T., and Uchiyama, A, 1992, "Behaviors of the Laterally Injected Jet in Film Cooling: Measurements of Surface Temperature and Velocity/ Temperature Field Within the Jet," ASME Paper No. 92-GT-180.

Ligrani, P. M., Ciriello, S., and Bishop, D. T., 1992, "Heat Transfer, Adiabatic Effectiveness, and Injectant Distributions Downstream of a Single Row and Two Staggered Rows of Compound Angle Film Cooling Holes," ASME *Journal of Turbomachinery*, Vol. 114, pp. 687-700.

Makki, Y. H., and Jakubowski, G. S., 1986, "An Experimental Study of Film Cooling from Diffused Trapezoidal Shaped Holes," AIAA Paper No. AIAA-86-1326.

Pedersen, D. R., Eckert, E. R. G., and Goldstein, R. J., 1977, "Film Cooling with Large Density Differences Between the Mainstream and the Secondary Fluid Measured by the Heat-Mass Transfer Analogy," ASME *Journal of Heat Transfer*, Vol. 99, pp. 620-627.

Pietrzyk, J. R., Bogard, D. G.,and Crawford, M. E., 1990, "Effects of Density Ratio on the Hydrodynamics of Film Cooling," ASME *Journal of Turbomachinery*, Vol. 112, pp. 437-443.

Sathyamurthy, P., and Patankar, S.V., 1990, "Prediction of Film Cooling with Lateral Injection," AIAA/ASME Thermophysics and Heat Transfer Conference, Seattle, WA.

Sen, B., Schmidt, D.L., and Bogard, D.G., 1994, "Film Cooling with Compound Angle Holes: Heat Transfer," submitted to the 1994 ASME International Gas Turbine Conference, The Hague, Netherlands.

Sinha, A. K., Bogard, D. G., and Crawford, M. E., 1991, "Film Cooling Effectiveness Downstream of a Single Row of Holes with Variable Density Ratio," ASME *Journal of Turbomachinery*, Vol. 113, pp. 442-449.

Thole, K. A., Sinha, A. K., Bogard, D. G., and Crawford, M. E., 1992, "Mean Temperature Measurements of Jets with a Crossflow for Gas Turbine Film Cooling Application," Rotating Machinery Transport Phenomena, J.H. Kim and W.J. Yang, ed., Hemisphere Pub. Corp., New York.